Quantum Dynamic Approach of $B_2N^{(\mp,0)}$ and $N_2B^{(\mp,0)}$ Clusters Study: A Symmetry Breaking due to the JAHN-TELLER Effect

Majid Monajjemi * and Fatemeh Mollaamin

Posted Date: 18 April 2023

doi: 10.20944/preprints202304.0504.v1

Keywords: Boron nitride; B2N(∓,0); N2B(∓,0); JAHN-TELLER; Symmetry Breaking.

Article

Quantum Dynamic Approach of $B_2N^{(\mp,0)}$ and $N_2B^{(\mp,0)}$ Clusters Study: A Symmetry Breaking Due to the JAHN-TELLER Effect

Majid Monajjemi [1,*] and Fatemeh Mollaamin [2]

[1] Department of Chemical engineering, Central Tehran Branch, Islamic Azad University, Tehran, Iran
[2] Department of Biomedical Engineering, Faculty of Engineering and Architecture, Kastamonu University, Kastamonu, Turkey; smollaamin@gmail.com
* Correspondence: author: maj.monajjemi@iauctb.ac.ir

Abstract: BN compounds play an important role in the preparation of hyper- thin films, that have received signifcant attention in products. In this article, we investigated the electronic structures of $B_2N^{(\mp,0)}$ and $N_2B^{(\mp,0)}$. Triatomic NBN and BNB have recently been studied using various experimental and calculation approaches, and it is totally agreed that both of them are linear in their ground electronic step. The six ions including $B_2N^{(-)}$, $B_2N^{(+)}$, $B_2N^{(0)}$, $BN_2^{(-)}$, $BN_2^{(+)}$ and $BN_2^{(0)}$ have been studied and been also compared with one another in terms of several basis sets and predication of the symmetry breaking (SB) subject. Artifactual SB with the v_3 vibration is occurred in the *trial* wave functions of coupled-cluster level, even when Brueckner orbitals of all nitrogen and oxygen atoms are used. In the $D_{\infty h}$ of $B_2N^{(\mp,0)}$ and $N_2B^{(\mp,0)}$ molecules, the unpaired electrons are delocalized, while in the asymmetric $C_{\infty v}$, they are localized on either one of the B atoms or N atoms of $B_2N^{(\mp,0)}$ and $N_2B^{(\mp,0)}$, respectively. Structures with (SB), $C_{\infty v}$, can be stronger by interaction to the $D_{\infty h}$. Hereby, the second-order Jahn-Teller effect allows the unpaired electron to localize on boron atom, rather than being delocalized. Finally, from a statistical thermodynamical analysis, we calculated the thermodynamically stabilities of those six ions.

Keywords: Boron nitride; $B_2N^{(\mp,0)}$; $N_2B^{(\mp,0)}$; JAHN-TELLER; Symmetry Breaking

1. Introduction

1.1. *The structure of boron nitride clusters*

It is generally agreed that BNB and NBN are linear in their electronic states, but the controversy as to whether their geometries are symmetric or asymmetric have not yet been definitively settled [1-10]. Six ions including $B_2N^{(-)}$, $B_2N^{(+)}$, $B_2N^{(0)}$, $BN_2^{(-)}$, $BN_2^{(+)}$ and $BN_2^{(0)}$ compounds have been studied as the most complex items of (SB), both real and artifactual, due to pseudo second-order Jahn–Teller effect. Although various experimental or theoretical investigations were done for these issues [7-10], there are no quantum reports of this phenomenon through various basis sets calculation [11- 19]. Paldus [9] investigated the molecular system of $B_2N^{(0)}$ through multi-reference coupled cluster optimization with *RMR* Hamiltonian *& CCSD (T)* using cc-*pVNZ*, (N=2-5). In other approaches of CCSD (T), method, it has been also exhibited an asymmetric configuration of unequal BN bound length [1, 3]. $B_2N^{(0)}$ structure has been approved by Raman technique [4] which can be also synthesized according to the $B(^2P) + N(^4\,S) \rightarrow BN(^1\Sigma^+)$ and $B(^2P) + BN(^1\Sigma^+) \rightarrow BNB(^2\Sigma^+_{(u)})$ reactions [12]. The mathematical extrapolation suggested by Schlegel for the PMP4 calculation can be arranged as: $E_{PMP4\approx}E_{UMP4} + E_{PMP3} - E_{UMP3}$ and $E_{\infty} \cong \frac{E_2+E_3}{1-\frac{E_4}{E_2}}$. The related optimized parameters are also confirmed based on Figure1. The UHF/6-31G* calculation for spin expectation for <S²> are collected in Table 1 and Figure 1.

An accurate work on the electronic structure of $B_x\,N_{3-x}$ (x = 1, 2) was exhibited by *Martin et al* [1, 3, 5, 7 and 10] using both theoretical spectroscopic measurements.

Table 1. Electronic configurations and expectation values for <S²> by casscf/cc-pvxz (x=3) level of theory

Preprints (www.preprints.org) | NOT PEER-REVIEWED | Posted: 18 April 2023 doi:10.20944/preprints202304.0504.v1

Item	*molecule*	*Point group*	*Term*	$< S^2 >^a$	$< S_1^2 >^b$	$< S_A^2 >^c$	Electronic configuration
(a)	B_3	$D_{\infty h}$	$^2\Pi_g$	1.80	1.80	0.84	$(\sigma_g)^2(\sigma_u)^2(\sigma_g)^2(\sigma_g)^2(\sigma_u)^2(\sigma_g)(\sigma_u)(\pi_u)^3$
(b)	B_3	$D_{\infty h}$	$^4\Pi_u$	3.80	3.75	3.70	$(\sigma_g)^2(\sigma_u)^2(\sigma_g)^2(\sigma_g)^2(\sigma_u)^2(\sigma_g)(\sigma_u)(\pi_u)^3$
(c)	BN_2	$C_{\infty v}$	$^2\Pi_g$	0.85	0.80	0.75	$(\sigma)^2\,(\sigma)^2\,(\sigma)^2\,(\sigma)^2\,(\sigma)^2\,(\sigma)^2\,(\pi)^4\,(\sigma)^2\,(\pi)$
(d)	BN_2	C_s	$^4A_2$	1.35	1.30	0.90	$(a')^2\,(a')^2\,(a')^2\,(a')^2\,(a')^2\,(a')^2\,(a')^2\,(a'')^2$ $(a')^2\,(a')^2\,(a'')^2$
(e)	BN_2	$D_{\infty h}$	$^2\Pi_g$	0.90	0.90	0.81	$(\sigma_g)^2(\sigma_u)^2(\sigma_g)^2(\sigma_g)^2(\sigma_u)^2(\sigma_g)^2(\pi_u)^4\,(\sigma_u)^2$ (π_g)
(f)	B_3	$D_{\infty h}$	$^2\Pi_g$	1.80	1.80	0.85	$(\sigma_g)^2(\sigma_u)^2(\sigma_g)^2(\sigma_g)^2(\sigma_u)^2(\sigma_g)\,(\sigma_u)\,(\pi_u)^3$
(g)	B_3	$D_{\infty h}$	$^4\Pi_g$	3.80	3.80	3.70	$(\sigma_g)^2(\sigma_u)^2(\sigma_g)^2(\sigma_g)^2(\sigma_u)^2(\sigma_g)\,(\sigma_u)\,(\pi_u)^3$
(h)	BN_2	C_{2v}	^2A_g	1.40	1.30	1.10	$(a_1)^2\,(b_1)^2(a_1)^2(a_1)^2(b_2)^2(a_1)^2(b_1)^2$ $(b_2)^2(a_1)^2(a_2)$
(i)	B_2N	$C_{\infty v}$	$^2\Sigma_g^+$	2.30	2.25	2.60	$(\sigma)^2\ (\sigma)^2\ (\sigma)^2\ (\sigma)^2\ (\sigma)^2\ (\sigma)^2\ (\sigma)\ (\pi)^4$ $(b_1)^2(b_2)^2(a_1)^2$
(j)	B_2N	$C_{\infty v}$	$^4\Sigma_g^+, \Sigma_g^-, \Delta$	4.00	4.00	3.74	$(\sigma)^2\,(\sigma)^2\,(\sigma)^2\,(\sigma)^2\,(\sigma)^2\,(\sigma)^2\,(\pi)^3\,(\sigma)\,(\pi)$
(k)	BN_2	C_{2v}	$^4B_1$	3.80	3.80	3.70	$(a_1)^2\ \ (b_2)^2(a_1)^2(a_1)^2(b_2)^2(a_1)^2(b_1)^2$ $(a_1)^2(a_1)\ (b_2)\ (a_2)$

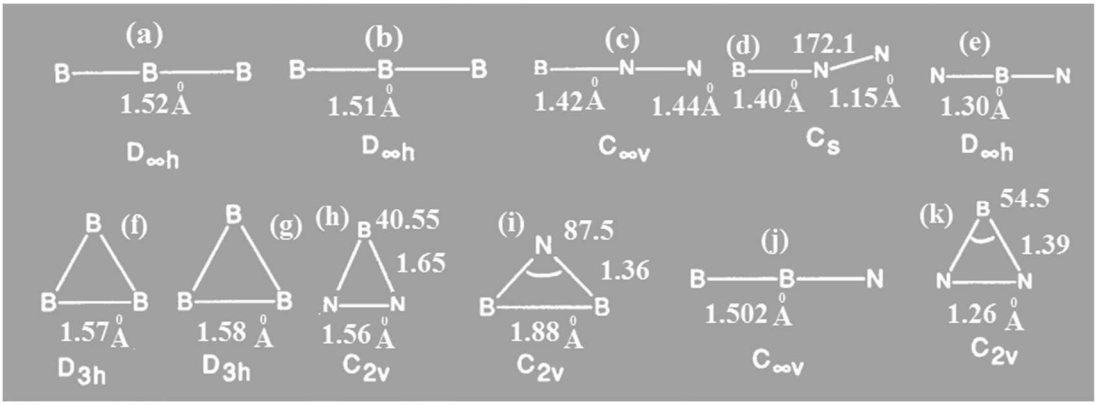

Figure1. Stationary points for BN_2, NB_2, and B_3 ; Bond distances in Angstrom units.

Asmis [2] confirmed the ground state structure of B_2N^- both by photoelectron analysis and theory and indicated its electronic configuration as ($\tilde{X}^1\sum_g^+$). He also demonstrated the situation of $B_2N^{(0)}$ ($\tilde{X}^2\sum_u^+$) and ($\tilde{A}^2\sum_g^+$) in excited state by a linear symmetry combination as reaction as follows; $\tilde{X}^1\sum_g^+ \rightarrow \tilde{X}^2\sum_u^+ + e^-$ and $\tilde{X}^1\sum_g^+ \rightarrow \tilde{A}^2\sum_g^+ + e^-$. In other side, the IR data exhibited a spectrum at 6000 cm^{-1} in $\tilde{A}^2\sum_g^+ \rightarrow \tilde{X}^2\sum_u^+$ [7, 8]. The Walsh's idea [17] confirmed all $BN^{(-,0,+)}$ variants of ($\tilde{X}^2\sum_u^+$) to ($\tilde{X}^1\sum_g^+$) for $B_2N^{(0)}$ and B_2N^-, respectively.

Löwdin [18] exhibited; such broken-symmetry (BS) usually has a lower energy compared with the symmetry-adapted (SA). It is notable the SB phenomenon, is due to the restricted hartree fock or in opposite the ROHF potential energy surfaces (PESs) for the linear ABA type (Such as NB_2 or BN_2). Wigner [19] confirmed that the Pauli principle and being simultaneously an Eigen function of $<S^2>$ and $<S_Z>$ can be written as: $\psi_{S,M}(\overrightarrow{x_1}, \overrightarrow{x_2}, \ldots\ldots \overrightarrow{x_N}) = (\sqrt{f_N^S})^{-1}\sum_{i=1}^{f_N^S}\Phi_i\,(\overrightarrow{r_1}, \overrightarrow{r_2}, \ldots\ldots \overrightarrow{r_N})\Theta_i(\sigma_1, \sigma_1, \ldots\ldots \sigma_N)$.

Where, Φ_i is the spinless Schrödinger equation and Θ_i is spin eigenfunctions, and f_N^S is the number of spin Eigen-functions [19]. In this article, we focus on the $<S_z>$ and $<S^2>$ quantum numbers of various BN compounds (Table1).

1.2. *Thermochemical Considerations*

Seifert et al.[20] Calculated the physical and chemical properties of boron-nitrogen clusters based on thermochemical studies. For B2N, basically 3 different structures can be written as: BBN → B2 + N; (b) BBN→B + (BN); (c) BNB→(BN) + B. For BN2, the following three fragmentation reactions were considered: (a) BNN→B + N2; (b) BNN→(BN) + N; (c) NBN →(BN) + N. It is confirmed generally, BNN should be stronger than NBN, and in the other side, BNB will be more stable than NBB. This is

Preprints (www.preprints.org) | NOT PEER-REVIEWED | Posted: 18 April 2023 doi:10.20944/preprints202304.0504.v1

in agreement with the data, that B2N is appeared in mass spectra, while BN2 is not. We also calculated the thermochemical properties of our model based on Seifert work.

1.2. Potential energies surfaces (PESs)

PESs of linear triatomic XYX has been done for the cutting along the symmetrical and asymmetrical stretching modes. We mentioned the linear of X-Y and Y-X as R1 and R2, respectively. Cutting of the symmetrical stretching is oriented by the parameters same as R =R1=R2, and the energy minimum on the PEC E(R) describes the symmetrical optimized for R=Re. We also define these stretching coordinates as: Δ(R)=R1-R=R-R2. As well as the two PECs, defined by E(R) and E [Δ(R)] , along the R and Δ orientation, respectively. Consequently, the PEC has been labeled as E(R) or V (R) for the symmetrical stretching form and as well as the E [Δ(R)] or V [Δ(R)] has been defined for the asymmetric al form. (Figure 2).

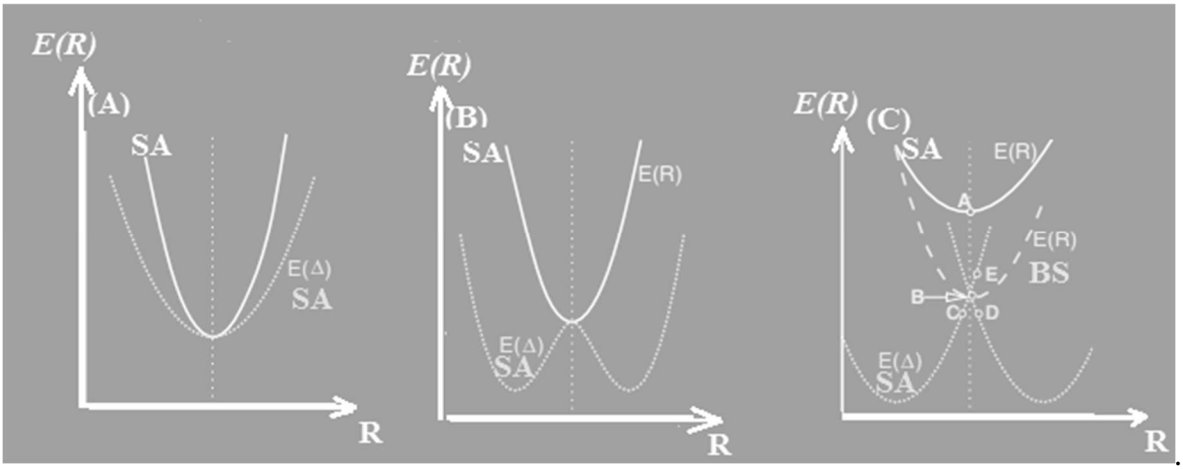

Figure2. The cuts of the PES along the symmetric ® and asymmetric (Δ) stretching by E(R) and E(Δ), respectively.

2. Computational details and Methods

CASSCF wave functions have been accomplished as a basic calculation for estimating the energies along the BN–B coordinating changes. Since the definition of active space is needed for the CASSCF wave function, all the valence orbitals of the constituent atoms, i.e., 2*s* 12*p* have been considered clearly. EPR-III (and II) basis sets of Barone's model [21] shown the most compatible data for electrostatic potential fitting (ESP).

The EPR(II) is a double-ζ basis set with polarization for B to F [21, 22] that is needed for $\mathbf{N_2}B^{(\mp,0)}$ $\mathbf{B_2}N^{(\mp,0)}$ calculation. EPR(III) is also a triple-ζ including diffuse parameter, of d-orbital, and compared with EPR(II), s-part improved for better energy minimization [20-24].

The correlation of valence basis sets have been investigated by Dunning and coworkers, named by cc-pV*x*Z, where *x* =2, 3, 4, 5 & 6 where used in this work. Additionally, these are includes of basically contracted sets of [3*s*2*p*1*d*] (cc-pVDZ), [4*s*3*p*2*d*1*f*] (cc-pVTZ), [5*s*4*p*3*d*2*f* 1*g*] (cc-pVQZ), and [6*s*5*p*4*d*3*f* 2*g*1*h*] (ccpV5Z) that are constructed through adding shell layers orbitals of *s*,*p*,*d*,... to the atomic Hartree–Fock wavefunction. Moreover, the polarization factors, which increase from 1d-cc-pVDZ to 4*d*-cc-pV5Z are added.

In other sides, the active space for the CASSCF (active electrons / active orbitals) should be defined for all valence orbitals in the post HF methods, such as 11/ 12 for $B_2N^{(0)}$ and 10/ 12 for $B_2N^{(+)}$ and so on.

The various basis sets in their effect to **symmetry breaking of** artifactual or trial wave function, the $\mathbf{B_2}N^{(\mp,0)}$ have been optimized through several level of theories such as CASSCF(11/12)/ccPVQZ for $\mathbf{B_2}N^{(-)}$, CASSCF(11/12)/AUG-ccPVTZ for $\mathbf{B_2}N^{(0)}$ and CASSCF (10/12)/ccPVTZ for $\mathbf{B_2}N^{(+)}$ [25, 26]. For this purpose, the self correlation consistent orbitals are well increased both in size and accuracy to converge systematically. The augmented functional sets are used from cc-pV*N*Z (N=2-6)

Preprints (www.preprints.org) | NOT PEER-REVIEWED | Posted: 18 April 2023 doi:10.20944/preprints202304.0504.v1

by the addition of a single diffuse orbitals for the anions and in other hand for each item, only the polarization orbitals were used. The configuration interaction (CI) including single and double items [27] have been also used for estimating several physical parameters such as natural bounding orbital (NBO), Atoms in molecules by Bader (AIM) [28], NPA or natural population analysis, electrostatic potentials, and electrostatic potential-derived charge using the Merz-Kollman-Singh[29], chelp[30], or chelpG[31]. The Hyperpolarizability has been calculated via CISD, QCISD, MP_2 and CASSCF levels of calculations. The AIM of Bader's theory was used for measuring the critical point maps to predict the atomic behaviors in $\mathbf{B_2}N^{(\mp,0)}$ species [28].

The atomic charges can be computed over several species of $N_2B^{(\mp,0)}$ and $B_2N^{(\mp,0)}$ using abinitio quantum chemical packages such as Gaussian or GAMESS-US [32]. The potential surfaces(PS) of B_2N and BN_2 have been studied using the post Hartree Fock methods, such as CASSCF, MP4, PMP4, and QCISD. Spin contamination is shown to present severe problems with the MP4SDQ procedure.

3. Results and Discussion

3.1. Molecular orbital description

3.1.1. $\mathbf{B_2N^{(\mp,0)}}$

Definition of the PS was exhibited to be not entirely enough at the UHF, more not qualitatively. In our calculation B_2N variants mostly are found to have a symmetric linear coordination in its ground state($\tilde{X}\,^2\sum_u^+$). Sometimes the asymmetric linear structure possibly being appeared a small amounts at higher temperatures. The $\mathbf{B_2}N^{(0)}$ configuration term of ground state ($\tilde{X}\,^2\sum_u^+$) with electrons occupancy with the lowest excited state is:$1\sigma_g^2, 1\sigma_u^2, 2\sigma_g^2, 3\sigma_g^2, 2\sigma_u^2, 1\pi_u^4, 4\sigma_g^2, 3\sigma_u^1$ that predicted to be $\tilde{A}^2\Sigma_{(g)}^+$, with an orbital occupancy of$1\sigma_g^2, 1\sigma_u^2, 2\sigma_g^2, 3\sigma_g^2, 2\sigma_u^2, 1\pi_u^4, 4\sigma_g^1, 3\sigma_u^2$. In addition, $\tilde{B}^2\Pi_g$ exited state can be written $1\sigma_g^2, 1\sigma_u^2, 2\sigma_g^2, 3\sigma_g^2, 2\sigma_u^2, \pi_u^4, 4\sigma_g^2, 1\pi_g^1$ (above the$\tilde{A}\,^2\Sigma_g^+$) is subject to the Renner-Teller effect and further exited state depends on the ($^4\Pi_g$) of triplet form. The electron Configuration energies of $B_2N^{(\mp,0)}$ both in **ground and exited states**, with HOMO/LUMO amounts are listed in Table 2.

Table 2. Geometries and electrical properties of $B_2N^{(0)} = 17e$, $B_2N^{(-)} = 18e$ **and** $B_2N^{(+)} = 16e$ **in ground and exited states**

State (*N_e)	$E_e(Hartree)$	Total Configuration (Energy of $\|\alpha\rangle$ * $(Homo - Lumo)$**	βConfiguration Energy of $\|\beta\rangle$ * Beta virtual**	$r_e(B_1N)$ $r_e(NB_2)$	$A_1(2,1,3,-2,-1)$ A_2 $(2,1,3,-1,-2)$
$\tilde{X}\,^2\Sigma^+$ $(C_{\infty v})$ (*17e)	-104.078196^a $-104.082033^{a'}$ $-104.075492^{a''}$	$[\boldsymbol{A}], \pi^4, \sigma^2, \sigma^1\|\alpha\rangle$ $= -0.44641^a$ $* E(\|\alpha\rangle)(-34.87083)^a$ $** (-0.48614)^a$	$[\boldsymbol{B}]\sigma^1\|\beta\rangle$ $= -0.26180^a$ $* (-34.15046)^a$ $** (-0.17697)^a$		
$\tilde{X}\,^2\Sigma_u^+$ $(D_{\infty h})$ (*17e)	-103.639678	$[\boldsymbol{A'}]\pi_u^4, 4\sigma_g^2, 3\sigma_u^1\|\alpha\rangle$ $= -0.42477^d$ $* (-34.74888)^d$ $** (-0.49245)^d$	$[\boldsymbol{B'}], 4\sigma_g^1\|\beta\rangle$=- 0.24844^d $* (-34.06924)^d$ $**(-0.18742)^d$	1.3176^d 1.3176^d	$A_1 = 180.0^d$ $A_2 = 180.0^d$
$\tilde{A}\,^2\Sigma_g^+$ (*17e)	-104.104759^k $-104.078173^{k'}$	$[\boldsymbol{A'}]\pi_u^4, 4\sigma_g^1, 3\sigma_u^2\|\alpha\rangle$ $= -0.44638^u$ $* (-34.8744)^u$ $** (-0.48626)^u$	$[\boldsymbol{A'}]\pi_u^4, 4\sigma_u^1,$ $= -0.26134$ $* (-34.15408)$ $** (-0.17666)$	1.3154^k 1.3154^k	$A_1 = 180.0^k$ $A_2 = 180.0^k$
$\tilde{B}^4\Pi_g$ (*17e)	-104.029702^h -104.014117^a	$[\boldsymbol{A'}]\pi_u^4, \pi_g^2, \sigma_g^1\|\alpha\rangle$ $= -0.26899^h$ $* (-35.04484)^{\boldsymbol{h}}$ $* (-0.30125)^h$	$[\boldsymbol{A'}], \pi_u^2\|\beta\rangle$ $= -0.4965^h$ $* (-33.74801)$ $** (-0.50595)$	$* 1.3079^j$ $* 1.3079^j$	$* A_1 = 180.0^x$ $* A_2 = 180.0^x$
$\tilde{X}\,^1\Sigma_g^+$ (*18e)	-104.196567^a $-104.201914^{a'}$ $-104.195017^{a''}$	$[\boldsymbol{A'}]1\pi_u^4, 4\sigma_g^2, 3\sigma_u^2$ $= -0.13904^a$ $* E(\|\alpha\rangle) = -32.48647^a$ $** -0.36286$		$* 1.335^y$ $* 1.335^y$	$A_1 =* 180.0^y$ $A_2 =* 180.0^y$
$\tilde{X}\,^1\Sigma_g^+$ (*18e)	-104.196566^b	$* E(\|\alpha\rangle) = -32.48644^b$		1.3291^b 1.3291	$A_1 = 180.0^b$ $A_2 = 180.0$

Preprints (www.preprints.org) | NOT PEER-REVIEWED | Posted: 18 April 2023 doi:10.20944/preprints202304.0504.v1

$\widetilde{B}\,^3\Sigma_g$ (*16e)	-103.760922^a -103.776711^h $-103.762855^{a'}$ $-103.759058^{a''}$	$\{[\boldsymbol{A'}]4\sigma_g^1, 3\sigma_u^1, \pi_u^4,\}^a$ $\pi_u^2\|\alpha\rangle = -0.74323^a$ $* E(\|\alpha\rangle)(-37.33372)^a$ $** (-0.53385)^a$	$\{[\boldsymbol{A'}], \pi_u^2\|\beta\rangle = -0.7522 * 1.2976^{\backprime} \; A_1 =* 180.0^w$ $* E(\|\beta\rangle)(-35.72475)^a * 1.2976^{\backprime} \; A_2 =* 180.0^w$ $** (-0.52131^a$

(a)QCISD/EPR-III;(**d**)CASSCF(11,12)/UHF;(**z**)b3p86/6-31g*;(**a'**)MP4D/EPR-III//QCISD/EPR-III; (**m**)CASSCF(10,12)/EPR-III(**x**)b3lyp/6-31g*;(**a''**)MP4SDQ/EPR-III//QCISD/EPR-III; (**g**)CASSCF(10,12)rohfAUG-cc-pvqz;(**y**)m062x/epr-ii;**(b)**QCISD/EPR-III([$\boldsymbol{A}$]: $1\sigma^2, 2\sigma^2, 3\sigma^2, 4\sigma^2, 5\sigma^2$; :(**w**)b3lyp/6-31g*;**(c)** QCISD/EPR-II [$\boldsymbol{A'}$]: $1\sigma_g^2, 1\sigma_u^2, 2\sigma_g^2, 3\sigma_g^2, 2\sigma_u^2$; (**v**)CASSCF(11,12)/AUG-cc-pvqz;(**c'**)MP4D/EPR-II//QCISD/EPR-II:[$\boldsymbol{B}$]: $\sigma^1, \sigma^1, \sigma^1, \sigma^1, \pi^2$; **(c'')**MP4SDQ/EPR-II//QCISD/EPR-II; **[$\boldsymbol{B'}$]:**$1\sigma_g^1, 2\sigma_g^1, 1\sigma_u^1, 3\sigma_g^1, 2\sigma_u^1, 1\pi_u^2$; **(f)** CBS-lq;
(**h**)QCISD(T)/EPR-III; **[C]:**$1\sigma_g^2, 1\sigma_u^2, 2\sigma_g^2, 3\sigma_g^2, 2\sigma_u^2, 4\sigma_g^2$; (**n**)CBS4O; (**u**) TD/EPR-II ;
(**k**) TD/EPR-III//QCISD (T)/EPR-III; (***K'***)TD/EPR-III//QCISD /EPR-III
; [$\boldsymbol{C'}$]: $1\sigma_g, 1\sigma_u, 2\sigma_g, 3\sigma_g, 2\sigma_u$; [**D]:**$1\sigma_g^2, 2\sigma_g^2 1\sigma_u^2, 3\sigma_g^2, 2\sigma_u^2$

Seifert confirmed that BNB molecule (Figure1.e.) is much more stable compared with BBN (Figure1.c), and that BNB will not dissociate automatically in BN + B or N. +B_2. Bent quartet B_2N ($^2B_4$) : $(a_1)^2(a_1)^2$ $(b_2)^2(a_1)^2(a_1)^2(b_2)^2(a_1)(b_1)^2(b_2)(a_1)$ is also found much more stable compared to other species due to the effect of polarization orbitals. Inspection of (<S>^{2}) denotes an excessive amount of spin contamination, actually increases, rather than decreases, spin contamination. Since B_2 is known to have a very low-lying ($\widetilde{X}\,^5\sum_u^-$) state besides the ground ($\widetilde{X}\,^3\sum_g^-$) state, this fact can be interpreted from connecting the ($\widetilde{X}\,^5\sum_u^-$) B_2 to the ^{4}S nitrogen atom. Indeed, a ($\widetilde{X}\,^6\sum_g^+$) state $B_2N(C_{\infty v})$;{$(\sigma)^2(\sigma)^2(\sigma)^2(\sigma)^2(\sigma)^2(\sigma)^2(\pi)^2(\sigma)$ $(\pi)^2$} was found to lie only 23.0 kcal mol^{-1} above the doublet state with high value of <S>^{2}. For the sextuplets contaminating $B_2N(C_{\infty v})$ ($\widetilde{X}\,^6\sum_g^+$), the dynamic correlation would be even smaller. Indeed, B_2N ($C_{\infty v}$) ($\widetilde{X}\,^2\sum_g^+$) lies 44.9 kcal mol^{-1} above $B_2N(C_{\infty v})$ ($\widetilde{X}\,^6\sum_g^+$) at the UMP4 level, and 69.1 kcal mol^{-1} at the PMP4 level. At this situation, B_2N has a symmetric linear ($D_{\infty h}$) structure with ($\widetilde{a}\,^2\sum_u^+$); ground state with bond distance 1.31 angstrom and frequency around 20201 cm^{-1} . It is notable that the B_2N ($\widetilde{a}\,^2\sum_u^+$);) can be stabilized by resonance configuration as follows:

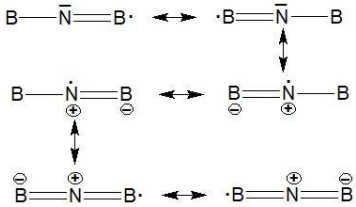

For the quartet state, the C_{2v} structure B_2N ($^2B_4$) will be most stable. It is isoelectronic with B_3 except for two unpaired ,while B_2N^- is isoelectronic with C_3).

3.1.2. $N_2\boldsymbol{B}^{(\mp,\mathbf{0})}$

Although our calculations confirm the more stability of BNN than NBN at the global minimum, at the casscf/ccpvxz (x=3, 4) levels, the linear quartet structures of BN_2 ($D_{\infty h}$) ($^4\Pi_g$) (Tables 1&2) exhibited an symmetrical structure, while ($C_{\infty v}$) ($^4\Sigma_g^-$) shown asymmetrical situation and are predicted to be most stable. At the casscf/cc-pvxz (x=4,5) levels on the other hand, the BN_2 ($D_{\infty h}$)($^4\Pi_g$) and ($C_{\infty v}$)($^4\Sigma_g^-$) is reversed and the bent doublet structure $^2B_2(C_{2v})$ is stabilized. During spin rotation, the symmetric linear doublet form of BN_2 ($D_{\infty h}$)($^2\Pi_g$) approaches towards ($C_{\infty v}$)($^4\Sigma_g^-$). In addition, an asymmetric linear doublet ($C_{\infty v}$)($^2\Pi_g$) can only be found after considerable amount, even with a lower energy by having a nonzero gradient on the bond angle. At the correlated optimization, BN_2 ($C_{\infty v}$)($^2\Pi_g$) convert to be the most stable structure at this point and through spin rotation, BN_2 ($D_{\infty h}$)($^2\Pi_g$) has only a little different with above items. Both of them are due to RennerTeller effect that theire frequencies are imaginary. As it can be seen in Table 2, a lower energy exists for BN_2 ($D_{\infty h}$)($^2\Pi_g$) at the Hartree-Fock level and also the Hartree fock frequencies may give imaginary variables due to the problem with ($C_{\infty v}$)($^2\Pi_u$) too. At the MP4SDQ/EPR-II//QCISD/EPR-II levels (Table 2), the bent structure is less stable that the linear one. At the MP4SDQ/EPR-III//QCISD/EPR-III levels, the Hartree-Fock result is confirmed at the PMP4 level. At both the CASSCF (11, 12)/UHF levels, the linear structure becomes distinctly more stable, by 6.5 and 6.1 kcalmol^{-1}, respectively. It is remarkable that the BN_2 ($D_{\infty h}$)($^2\Pi_g$) can be stabilized by resonance configuration as follows:

Preprints (www.preprints.org) | NOT PEER-REVIEWED | Posted: 18 April 2023 doi:10.20944/preprints202304.0504.v1

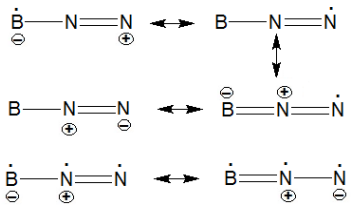

The lowest-lying states Renner-Teller distortions, harmonic frequencies, IR, and Raman are listed in Table 3.

Table 3. Harmonic frequencies, IR intensities and Raman activities of the most important clusters.

			ν3			ν3			ν2			
Item	Point group	Term	cm^{-1}	IR	Ram an	cm^{-1}	IR	Raman	cm^{-1}	IR	Ra man	E_{sp} $(kcal.mol^{-1})$
B_2N	$C_{\infty v}$	$^2\Sigma_g^+$	229	9	23	229	9	23	1355	12	10	4.08
B_2N	$D_{\infty h}$	$^2\Sigma_u^+$	78	4	0	229	9	23	1122	0	4	4.87
BN_2	$C_{\infty v}$	$^2\Pi_u$	111	12	15	244	10	7	907	12	10	4.45
BN_2	C_s	$^2A_1^{''}$	109	-	-	287	15	6	944	35	23	4.76
BN_2	C_v	$^4\Sigma_u^-$	85	2	3	400	1	3	1132	15	16	4.23
BN_2	$D_{\infty h}$	$^2\Pi_g$	-	-	-	176	19	0	1565	17	9	4.79
BN_2	C_{2v}	$^2A_1'$	-	-	-	102	-	-	1653	78	14	3.54
BN_2	C_{2v}	$^2A_2'$	-	-	-	1088	1	5	1432	14	54	5.01
BN_2	C_{2v}	$^2B_1'$	-	-	-	-	-	-	1343	18	52	3.99

3.2. Thermochemical studies of B2N and BN2

The concerned formulas are exhibited in many textbooks of statistical quantum thermodynamics; expressions may also be found Herzberg book [33, 34] that was used in the present work. Table 4 data exhibit the calculated energies of related reaction at the MP4/6-31G*, PMP4/6-31G*, CCD/6-31G*, and CCD + ST(CCD)/6-31G* levels, along with the LCAO-LDA.

Table 4. Energies (kcal mol^{-1})of boron nitried reactions at various levels.

Reaction	MP4D/EPR-III// QCISD/EPR-III	QCISD/ EPR-III	CASSCF(10,12) /EPR-III	TD/EPR-III// QCISD	QCISD/ EPR-II	CBS-lq
$B_2N \longrightarrow BN + B$	6.44	5.34	5.74	5.03	4.99	4.87
$B_2N \longrightarrow B_2 + N$	7.35	7.12	7.24	6.99	6.04	5.99
$BN_2 \longrightarrow BN + N$	4.91	4.21	4.33	4.38	4.33	4.21
$BN_2 \longrightarrow N_2 + B$	0.15	0.18	0.16	0.19	0.21	0.09

Comparing the quantities optimization of Seifert *et al.* with our data in this work, it is confirmed that BNB {$(D_{\infty h})$ $(^2\Sigma_g^-)$ } is much more stable than BBN ($(C_{\infty v})$ $(^2\Sigma_g^+)$), and therefore BNB will not dissociate automatically in either BN + B or B_2 + N.

3.3. Quantum symmetry breaking of $N_2B^{(\mp,0)}$ *and* $B_2N^{(\mp,0)}$ *and partial charges*

One of the targets of this work is to illustrate the difference among the electromagnetic situation of the $B_2N^{(\mp,0)}$ species due to changing basis sets and methods and also the **quantum SB report due to** trial wave function. In $D_{\infty h}$ position of$B_2N^{(\mp,0)}$, the unpaired electron is delocalized, while in the asymmetric$C_{\infty v}$, it is localized on either one of the B atoms. C∞v by SB structure becomes stronger

Preprints (www.preprints.org) | NOT PEER-REVIEWED | Posted: 18 April 2023 doi:10.20944/preprints202304.0504.v1

through changing to$D_{\infty h}$. Based on quantum chemistry theories, the second-order Jahn-Teller effect allows the unpaired electron to localize on boron atom, rather than being delocalized (Table 2 and Figure 3-a and 3-b).

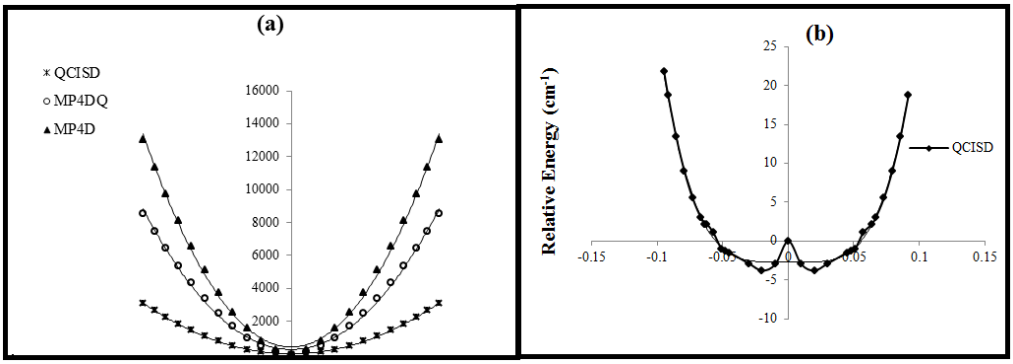

Figure 3. The $B_2N^{(-,0,+)}$ **relative energies versus** B-N-B bond distance in (a) for cation, (b), for radical.

The unpaired electron of nitrogen in $B_2N^{(0)}$ ($D_{\infty h}$) is delocalized and it is localized in the asymmetric ($C_{\infty v}$) for both of$B_2N^{(,0)}$and $B_2N^{(-)}$ species. Moreover, there is a restriction for the unpaired electron of nitrogen of BNB for delocalization between $D_{\infty h}$ and $C_{\infty v}$ symmetries states. These limitations between localized and non-localized situations increase the SB effect of the $B_2N^{(\mp,0)}$species. Meanwhile, ESP, forces, $\gamma = (V_B - V_N)/r_{BN}$, attraction and repulsion energies (eV) of $B_2N^{(\mp,0)}$ in ground and exited states are listed in table 2. The MESP fitting for $B_2N^{(,0)}$ and the summation of partial charges for two boron and one nitrogen ($B^{\delta q_1}-N^{\delta q_2}-B^{\delta q_3}$) in all models from $\Delta = 0.0\ to\ 0.07$ are zero (Table 2). Obviously, the summation of partial charges in $B^{\delta q_1}-N^{\delta q_2}-B^{\delta q_3}$ for $B_2N^{(0)}$radical is not 0.0 and it has changed according to: (0.23+0.23+0.52=0.98) for$\Delta^u = 0.0$, (0.24+0.23+0.52=0.99) for$\Delta^u = 0.02$. The changes among $\Delta^u, \Delta^k$and Δ^x is due to various methods and basis sets that are used in our work. Certainly, it is related to the the summation of partial charges in $B_2N^{(0)}$ radical that is far from 0.0 and varies between 0.00 and 0.16. It could be due to the fact that the unpaired electron of nitrogen is localized while $B_2N^{(-)}$ is under the influence of the unpaired electron.

Interestingly, for the exited state of$B_2N^{(0)}$, changing of MESP for both exited and ground states of($\tilde{B}^4\Pi_g$), ($\tilde{X}^2\sum_u^+$), respectively are small. The sum of partial charges (in$B^{\delta q_1}-N^{\delta q_2}-B^{\delta q_3}$) for all items from $\Delta = 0.0$ to $\Delta = 0.2$ are -1, however, the total partial charges of $B^{\delta q_1}-N^{\delta q_2}-B^{\delta q_3}$ for $B_2N^{(-)}$ are not -1. The nitrogen of $B_2N^{(-,+,0)}$ is always positive for radical and anion and negative for cation, while in exited states, the sum of partial atomic charges are positive for all three forms. As it can be seen in Figure 4, radical or anion $B_2N^{(-,0)}$ has not been appeared from these kind calculation, though, for cation, there is a critical point at 90° for MP4DQ and MP4DSQ methods.

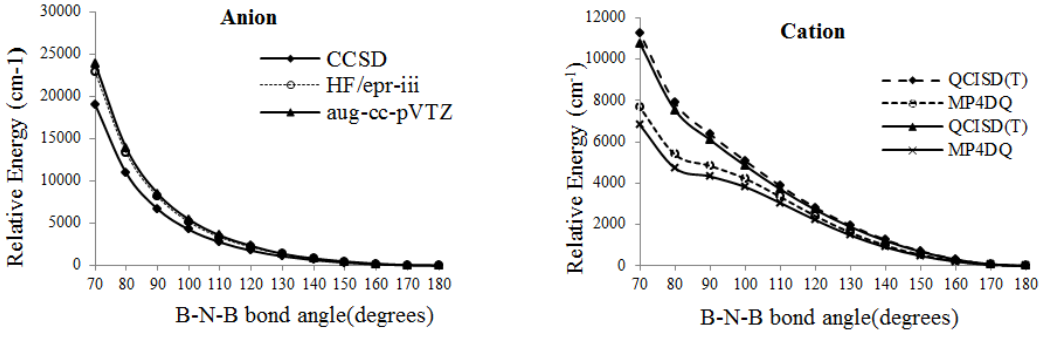

Figure 4. Relative energies of $B_2N^{(-,+)}$ **versus** B-N-B bond angle in various levels of theory.

From the SCF calculation, the minimum energy related to a bent structure with an angle around 90°, however, for the QCISD(T), MP4DQ, MP4DSQ and HF/aug-cc-pVTZ calculations (Figure 2), the

Preprints (www.preprints.org) | NOT PEER-REVIEWED | Posted: 18 April 2023 doi:10.20944/preprints202304.0504.v1

linear situation has the lowest energies for radical and anion . By consideration wave function, when the BNB has $D_{\infty h}$, the real wave-function might be converting as an irreducible representation of the $D_{\infty h}$. Table 5 presents data for the association enthalpy, entropy, and free energy from the statistical thermodynamic and partition functions, as well as values for the absolute entropy [35-44].

Table 5. Calculated thermodynamic properties at some selected temperatures.

Temperature (K)	$B_2N^{(-)}$	$BN_2^{(-)}$	$B_2N^{(+)}$	$BN_2^{(+)}$	$B_2N^{(0)}$	$BN_2^{(0)}$
Association enthalpy (kcal/mol)						
0	-266.5	-225.1	-208.5	-199.09	193.07	194.08
300	-266.1	-227.1	-211.4	-205.03	-201.05	-207.02
1000	-269.1	-228.9	-210.08	-205.96	-204.55	-203.63
20000	-269.8	-230.1	-203.05	-202.08	-205.01	-208.07
Free energy of association (kcal/mol)						
0	-264.92	-225.04	-206.99	-199.04	200.05	200.49
300	-247.97	-206.95	-192.05	-185.09	-203.05	-200.06
1000	-203.97	-160.08	-135.95	-131.40	-207.95	-202.91
20000	-139.95	-89.92	-65.04	-75.83	-204.09	-205.06

5. Conclusions

The potential surfaces of $B_2N^{(\mp,0)}$ and$N_2B^{(\mp,0)}$, have been studied using several post HF and basis sets methods. CASSCF optimization exhibited SB phenomenon for linear BNB containing an unequal bond length. We found for yielding accurate data doing perturbation theory (CASSCF+PT2) calculation and multi-reference (CI) with (CASSCF+1+2) wave functions are needed. In summary, we have clearly shown , where the SB problem is hidden , usual way to circumvent of peculiarities are the most important feature of this work. In particular, we find the low value for the anti-symmetric stretching fundamental frequency very encouraging, providing an additional support to the idea of actual symmetry breaking in the BNB ground state.

Author Contributions: Majid Monajjemi: Conceptualization and idea, Methodology, , Supervision. Fatemeh Mollaamin: Methodology, Software, Formal analysis, Investigation, Data Curation, Writing-review and editing, Visualization, Resources.

Funding: This research received no external funding.

Conflicts of Interest: The authors declare no conflict of interest.

References

1. J.M.L. Martin, J.-P. François, and R. Gijbels, Chem. Phys., **90**, 6469 (1989). doi: org/ 10.1063/1.456313.
2. K.R.Asmis, T.R.Taylor, and D.M. Neumark, J. Chem. Phys.**, 111**, 8838 (1999). doi: org/ 10.1063/1.480230.
3. J.M.L.Martin, J.-P.François, and R. Gijbels, Chem. Phys. Lett., **172**, 354 (1990). doi: org/10.1016/s0009-2614(90)87126-c.
4. L.B.Knight, Jr.D.W.Hill, T.J.Kirk, and C.A. Arrington, J. Phys. Chem., **96**, 5604 (1992). https://doi.org/10.1063/1.462703.
5. J. M. L.Martin, J.-P.François, and R. Gijbels, Chem. Phys. Lett. **193**, 243 (1992). doi: org/10.1016/0009-2614(92)85662-T.
6. P. Hassanzadeh, and L. Andrews, J. Phys. Chem. **96**, 9177 (1992). doi: org/10.1021/j100202a020.
7. L. Andrews, P. Hassanzadeh, T. R. Burkholder, and J. M. L. Martin, J.Chem. Phys. **98**, 922 (1993). doi: org/10.1063/1.464256.
8. C. A. Thompson, and L. Andrews, J. Am. Chem. Soc. **117**, 10125 (1995). doi: org/10.1021/ja00145a029.
9. X. Li, and J. Paldus, J. Chem. Phys. **126**, 224304 (2007). doi: org/10.1063/1.2746027.
10. J.M.L. Martin, J. El-Yazal, Mol. Phys. **85**,527 (1995). doi: org/10.1080/00268979500101281.

11. G.Meloni, M. Sai Baba, and A. Gingerich, J. Chem. Phys. **113**, 8995 (2000).doi: org/10.1063/1.1319353.
12. W. R. M. Graham, and W. Weltner Jr., J. Chern. Phys. *65*, 1516 (1976). doi: org/10.1063/1.433206.
13. M. Monajjemi, Chemical Physics. **425**, 29 (2013). doi: org/10.1016/j.chemphys.2013.07.014.
14. M.Monajjemi, V.S.Lee, M.Khaleghian, B.Honarparvar, F. Mollaamin, J. Phys. Chem. C, **114**, 15315 (2010). doi: org/10.1021/jp104274z.
15. M.Monajjemi, J.E. Boggs, J. Phys. Chem. A, **117**, 1670 (2013). doi: org/10.1021/jp312073q.
16. M. Monajjemi, Struct. Chem. **23**, 551 (2012). doi: org /10.1007 /s11224-011-9895-8.
17. L. Mahdavian, M. Monajjemi, Microelectronics journal, **41**, 142 (2010). doi: org/10.1016/j.mejo.2010.01.011.
18. Löwdin, P.O. Rev. Mod. Phys. **35**, 496 (1963). doi: org/10.1103/REVMODPHYS.35.724.
19. E. P. Wigner, Group Theory and its Application to the Quantum Mechanics of Atomic Spectra, Academic Press, New York, p. 259 (1959).
20. G. Seifert, B. Schwab, S. Becker, and H. J. Dietze, Int. J. Mass Spectr. Ion Proc. 85, 327 (1988).
21. V. Barone, Recent Advances in Density functional methods, parts I, Ed. D.P.Chong , world scientific publ. Co, springer, (1996**)**.
22. X.Blase, A.Rubio, S.G.Louie, and M.L. Cohen, Europhysics Letters (EPL), **28**, 335 (1994). doi: org/10.1209/0295-5075/28/5/007.
23. X. Blase, J.C. Charlier, A.de.Vita, R. Car, Appl. Phys. Lett. **70**, 197 (1997). doi: org/10.1063/1.118354.
24. W.Han, Y.Bando, K.Kurashima, and T. Sato, Appl. Phys. Lett. **73**, 3085 (1998). doi: org/10.1063/1.122680.
25. T.E.H. Walker, W. G. Richards, J.chem.phys. **52**, 1311 (1970). doi: org/10.1063/1.1673131.
26. S. Koseki, M.W. Schmidt, and M.S. Gordon, J.phys.chem. **96**, 10768 (1992). doi: org/10.1021/j100205a033.
27. J.A. Pople, M. Head-Gordon, and K. Raghavachari, J.chem.phys., **87**, 5968 (1987). https://doi.org/10.1063/1.453520.
28. R.F.W. Bader, Atoms in Molecule: A quantum Theory , Oxford Univ. press, Oxford, (1990).
29. B.H. Besler, K.M. Merz Jr., and P.A. Kollman, J. comp. Chem. **11**, 431 (1990). doi: org/10.1002/jcc.540110404.
30. L.E. Chirlian, and M.M. Francl, J.comp.chem. **8**, 894 (1987). doi: org/10.1002/jcc.540080616.
31. C.M. Breneman, and K.B. Wiberg, J. Comp.Chem. **11**, 361 (1990). doi: org/10.1002/jcc.540110311.
32. M. J. Frisch, G. W. Trucks, H. B. Schlegel, G. E. Scuseria, M. A. Robb, J. R. Cheeseman, G. Scalmani, V. Barone, G. A. Petersson, H. Nakatsuji, X. Li, M. Caricato, A. Marenich, J. Bloino, B. G. Janesko, R. Gomperts, B. Mennucci, H. P. Hratchian, J. V. Ortiz, A. F. Izmaylov, J. L. Sonnenberg, D. Williams-Young, F. Ding, F. Lipparini, F. Egidi, J. Goings, B. Peng, A. Petrone, T. Henderson, D. Ranasinghe, V. G. Zakrzewski, J. Gao, N. Rega, G. Zheng, W. Liang, M. Hada, M. Ehara, K. Toyota, R. Fukuda, J. Hasegawa, M. Ishida, T. Nakajima, Y. Honda, O. Kitao, H. Nakai, T. Vreven, K. Throssell, J. A. Montgomery, Jr., J. E. Peralta, F. Ogliaro, M. Bearpark, J. J. Heyd, E. Brothers, K. N. Kudin, V. N. Staroverov, T. Keith, R. Kobayashi, J. Normand, K. Raghavachari, A. Rendell, J. C. Burant, S. S. Iyengar, J. Tomasi, M. Cossi, J. M. Millam, M. Klene, C. Adamo, R. Cammi, J. W. Ochterski, R. L. Martin, K. Morokuma, O. Farkas, J. B. Foresman, and D. J. Fox, Gaussian 09, Revision A.02, Gaussian, Inc., Wallingford CT, (2016).
33. G. Herzberg, Infrared and Raman Spectra ofPolyatomic Molecules (Van Nostrand Reinhold, New York), p. 521 If. (1945).
34. Manual ofsymbols and Terminology for Physico-chemical Quantities and Units (prepared by M. L. McGlashan, revision prepared by M. A. Paul, second revision by D. H. Whilfen) , Pure Appl. Chern. **51**,1 (1979).
35. S. Bagheri, M.Monajjemi, A. Ziglari , A. Taghvamanesh ,Russian Journal of Physical Chemistry B, **15**, S140-S148 (2021), doi: org/10.1134/S1990793121090049.
36. M. A. Ashraf, Z. Liu & M. Najafi , Russian Journal of Physical Chemistry B, **14**, 217-221 (2020), doi: org/10.1134/S1990793120020189.
37. A. Yu. Shaulov, L. V. Vladimirov, A. V. Grachev, V. M. Lalayan, E. M. Nechvolodova, R. A. Sakovich, V. K. Skachkova, E. V. Stegno, L. A. Tkachenko, S. A. Patlazhan & A. A. Berlin, Russ. J. Phys. Chem. B, **14**, 183-189 (2020). doi:org/10.1134/S1990793120010157.
38. E.A. Lebedeva, S.A. Astaf'eva, T.S. Istomina, Russ. J. Phys. Chem. B, **16**, 316-322 (2022). doi: org/10.1134/S1990793122010109.
39. A.G. Korotkikh, I.V. Sorokin, E.A. Selikhova, V. A. Arkhipov, Russ. J. Phys. Chem. B, **14**, 592-600 (2020). doi :org/10.1134/S1990793120040089.
40. A.G. Korotkikh, I.V. Sorokin, V.A. Arkhipov, Russ. J. Phys. Chem. B, 16, 253-259 (2022). doi: org/10.1134/S1990793122020075.
41. Gerasimov, G. N. ; Gromov,V. F.; Ikim, M. I.; L. I. Trakhtenberg, Effect of Composition and Structure of Metal Oxide Composites Nanostructured on Their Conductive and Sensory Properties, *Russ. J. Phys. Chem.*, **2021**, *15*, 1072–1083. https://doi.org/ 10.1134/ S199079 31 21310018.

42. Kablov, V.F., Strakhov, V.L., Kaledin, V.O. *et al.* Mathematical Modeling of the Physicochemical Properties of a Heat-Shielding Material from Highly Filled Elastomers. *Russ. J. Phys. Chem. B* **2021**, *15*, 880–887. https://doi.org/ 10.1134/ S199079 31210 50043.
43. Sarvendra Kumar, Surbhi & Yadav, M.K. Optimized Molecular Geometries, Internal Coordinates, Vibrational Analysis, Thermodynamic Properties, First Hyperpolarizability and HOMO–LUMO Analysis of Duroquinone Using Density Functional Theory and Hartree–Fock Method. *Russ. J. Phys. Chem. B* **2021**, *15* (Suppl 1), S22–S31. https://doi.org/ 10.1134/ S1990793121090116.
44. Sakovich, R.A., Shaulov, A.Y., Nechvolodova, E.M. *et al.* Energy of Intramolecular Interactions and Structure of Metallophosphate Polycomplexes with Water Molecules and Nitrogen-Containing Compounds. *Russ. J. Phys. Chem. B* **2020**, *14*, 516–521. https://doi.org/10.1134/S1990793120030094.